



Seasonal variations in physical characteristics of aerosol particles at the King Sejong Station, Antarctic Peninsula

Jaeseok Kim¹, Young Jun Yoon^{1,*}, Yeontae Gim¹, Hyo Jin Kang^{1,2}, Jin Hee Choi¹, and Bang
Yong Lee¹

¹Korea Polar Research Institute, 26 Songdomirae-ro, Yeonsu-gu, Incheon 21990, South Korea

²University of Science & Technology (UST), 217 Gajeong-ro, Yuseong-gu, Daejeon 34113,
South Korea

*Correspondence to: Y.J. Yoon (yjyoon@kopri.re.kr)



Abstract

The seasonal variability of the physical characteristics of aerosol particles at the King Sejong Station in the Antarctic Peninsula was investigated over the period of March 2009 to February 2015. Clear seasonal cycles of the total particle concentrations (CN) were observed. The monthly mean CN_{2.5} concentrations of particles with a particle size larger than 2.5 nm were the highest during the austral summer with a mean of $1080.39 \pm 595.05 \text{ cm}^{-3}$ and were the lowest during the austral winter with corresponding values of $197.26 \pm 71.71 \text{ cm}^{-3}$. A seasonal pattern of the cloud condensation nuclei (CCN) concentrations coincided with the CN concentrations, where the concentrations were minimum in the winter and maximum in the summer. We also estimated values of fit parameter C and k based on measured CCN spectra. The values of C varied from 6.35 cm^{-3} to 837.24 cm^{-3} , with a mean of $171.48 \pm 62.00 \text{ cm}^{-3}$. The values of k ranged between 0.07 and 2.19, with a mean of 0.41 ± 0.10 . In particular, the k values during the austral summer were higher than those during the winter, indicating that aerosol particles are more sensitive to supersaturation ratio (SS) changes during the summer than they are during the winter. Furthermore, the effects of the origin and the pathway travelled by the air mass on the physical characteristics of aerosol particles were determined. The modal diameter of aerosol particles that originated from the South Pacific Ocean showed seasonal variations; $0.023 \mu\text{m}$ in the winter and $0.034 \mu\text{m}$ in the summer for the Aitken mode and $0.086 \mu\text{m}$ in the winter and $0.109 \mu\text{m}$ in the summer for the accumulation mode.



1. Introduction

Aerosol particles in the atmosphere may be emitted directly from various natural and anthropogenic sources (i.e., primary aerosol particles) or produced by gas-to-particle conversion processes (i.e., secondary aerosol particles). They influence local and global climates directly by scattering and
5 absorbing radiation and indirectly by acting as cloud condensation nuclei (CCN) or ice nuclei (IN) (IPCC 2013). The physical, chemical, and optical properties of atmospheric aerosol particles determine their impact on climate change. Although various studies on the effects of aerosol particles on climate change have been carried out, the direct and indirect climate effects are still unascertained (IPCC, 2013). Moreover, in order to understand the sources and the processes of the atmospheric aerosol
10 particles, there should be a need to have their long-term observations at different regions because aerosol particles vary temporally and spatially.

The Antarctic region is highly sensitive to climate changes due to complex interconnected environmental systems (e.g. snow cover, land ice, sea-ice, and ocean circulation) (Chen et al., 2009). Previous studies show that the Antarctic Continent and the Antarctic Peninsula have experienced
15 noticeable climate changes (Rignot et al., 2004; Steig et al., 2009; Pritchard et al., 2012; Schneider et al., 2012). The Antarctic Peninsula, in particular, has a warming rate of more than 5 times that of the other regions on earth (Vaughan et al., 2003; IPCC, 2013). The Antarctic climate system can be linked with aerosol particles by complex feedback processes that involve aerosol-cloud interactions. In addition, because there are less anthropogenic emission sources in Antarctica, it is a suitable place to
20 study the formation and growth processes of the natural aerosol particles. For these reasons, the observation of the physical properties in Antarctica, i.e., total particle concentrations, size distributions and concentrations of black carbon and activated CCN, is necessary.

Over the years, measurements of aerosol particles have been widely conducted at various stations in Antarctica; notably: Aboa (Koponen et al., 2003; Virkkula et al., 2007; Kyrö et al., 2013), Amunsen-
25 Scott (Arimoto et al., 2004; Park et al., 2004), Concordia (Järvinen et al., 2013), Halley (Rankin and



Wolff, 2003; Roscoe et al., 2015), Kohnen (Weller and Wagenbach, 2007; Hara et al., 2010), Maitri (Pant et al., 2011), Mawson (Gras, 1993), McMurdo (Hansen et al., 2001; Mazzera et al., 2001), Neumayer (Weller et al., 2015), Syowa (Ito, 1985; Hara et al., 2011b), and Troll (Fiebig et al., 2014). The Antarctic aerosol particles have been investigated with regard to their size distributions (Koponen et al., 2003; Belosi et al., 2012), optical properties (Shaw, 1980; Tomasi et al., 2007; Weller and Lampert, 2008), chemical compositions (Virkkula et al., 2006; Weller and Wagenbach, 2007; Asmi et al., 2010; Hara et al., 2011a), and mass concentrations (Mazzera et al., 2001; Mishra et al., 2004). Some studies focused on aerosol transport in the upper atmosphere (Hara et al., 2011b) and new particle formation (Järvinen et al., 2013; Kyrö et al., 2013; Weller et al., 2015). Although various studies have been performed, the measurements taken at the Antarctic Peninsula and the long-term observations of aerosol particles are still insufficient.

In this study, we continuously monitored the physical characteristics of aerosol particles at the Korean Antarctic station (King Sejong Station) in the Antarctic Peninsula from March 2009 to February 2015. Measurements for aerosol size distribution and concentrations of total aerosol number, black carbon (BC), and CCN were carried out using various instruments. The main aim of this study was to determine the seasonal variations of the physical properties of aerosol particles in the Antarctic Peninsula. In addition, the physical characteristics of aerosol particles that originated from the ocean and continent of the Antarctic region were investigated with air mass back-trajectory analysis.

2 Methods

2.1 Sampling site and instrumentation

Continuous observations of the physical properties of aerosol particles have been carried out since March 2009 at the King Sejong Station (62.22°S, 58.78°W) in the Antarctic Peninsula. Detailed information of the sampling site is given by Choi et al. (2008). In brief, the King Sejong Station is located on the Barton Peninsula of King George Island (KGI). The population density of KGI is higher than that of other regions in Antarctica due to the various research activities carried out from eight



permanent on-site stations. The observatory is located approximately 400 m southwest of the main buildings, which include the power generator and crematory of King Sejong Station. Thus, the northeastern direction (355°-55°) was designated as the local pollution sector because of the emissions from the power generator and crematory at the station. We therefore discarded data from the local
5 pollution sector to improve data quality, and data where BC concentrations were higher than 100 ng m⁻³ were also discarded. In this study, we present the analysed results of the physical characteristics of aerosol particles obtained during March 2009 to February 2015.

The physical characteristics of aerosol particles were continuously observed with various instruments that included two condensation particle counters (CPCs), an aethalometer, a cloud
10 condensation nuclei counter (CCNC), and a scanning mobility particle sizer (SMPS). The observation methods are shown in Fig. 1.

We used a laminar flow air sampling system for the sampling of aerosol particles. An aerosol inlet with a 10 cm diameter without a wind sector controller was placed on the roof of the observatory (Fig.
1). The total flow rate of the sample air was maintained at 150 lpm.

15 Total particle number concentrations were examined with two CPCs: a TSI model 3776 that measured particles > 2.5 nm in diameter and a TSI model 3772 that measured particles > 10 nm. Sample aerosol flow rates of CPC 3776 and CPC 3772 were 1.5 lpm and 1.0 lpm, respectively.

The aethalometer was used to measure the concentration of light absorbing particles at two wavelengths (370 and 880 nm). In this study, we used the results obtained by measuring light
20 absorption at 880 nm to determine the BC concentrations. The flow rate of the sample was constant at 5.0 lpm. The main purposes of measuring BC concentrations were to investigate long-range transport aerosol particles and to assess the influence exerted by local pollution.

To measure the CCN concentrations, a CCNC (DMT CCN-100) was used at five different supersaturation ratios (SS) (0.2, 0.4, 0.6, 0.8, and 1.0 %) and total flow rate of 0.5 lpm. The CCN
25 concentrations were decided by exposing aerosol particles at supersaturated conditions and then



counting only the number of only activated droplets with a detector. The sampling duration was set at approximately 5 min for each SS value (except the 0.2 % SS) before it was changed to the next SS value. For a 0.2 % SS, CCN concentrations were measured for 10 min because it required additional time to achieve stability after completing measurements at a 1 % SS.

5 Aerosol size distributions were continuously measured with the SMPS, which consisted of a differential mobility analyser (DMA), a CPC (TSI 3772), a control unit, an aerosol neutralizer (soft x-ray), and a data logging system. The resolution of scanning time was set to 120 s for mobility particle diameters from 0.01 to 0.30 μm . A closed sheath-air loop with a diaphragm pump in the control unit was used to maintain the sheath flow of DMA. The flow rate of sheath air of DMA was 10 lpm. The
10 ratio of aerosol flow to sheath flow of DMA was 1:10.

Besides, meteorological parameters including temperature, relative humidity (RH), wind speed (WS), wind direction (WD), pressure, and UV and solar radiation were also continuously monitored over the entire observation period.

15 **2.2 Back-trajectory analysis**

In order to associate the physical properties of aerosol particles to their source areas for the sampling periods, the air mass back trajectory analysis were conducted using the Hybrid Single-Particle Lagrangian Integrated Trajectory (HYSPPLIT) model (Stein et al., 2015) (<http://www.arl.noaa.gov/HYSPLIT.php>). For every 6 h period, 120-h air mass back trajectories were
20 analysed, ending at heights of 100m, 500m, and 1500m above the ground level of the sampling site. The results where the origin and pathway of the air masses for at least 12 h were similar at three different heights were used for the analysis in this study. Based on this analysis, we have classified the air mass into four groups according to their origin and pathway: two continental regions (South America and Antarctica) and two oceanic areas (South Atlantic and South Pacific Ocean), as are shown
25 in Fig. 2.



3 Results and Discussion

3.1 Meteorological conditions

Fig. 3 depicts monthly variations of the meteorological parameters measured from an automatic weather system (AWS) during the whole observation period. The temperature varied between $-19.5\text{ }^{\circ}\text{C}$ and $+5.8\text{ }^{\circ}\text{C}$, with a mean of $-2.4 \pm 2.1\text{ }^{\circ}\text{C}$ and the RH was between 60 % and 100 %, with a mean of $87.9 \pm 3.3\%$. As mentioned in previous studies (Kwon and Lee, 2002; Mishra et al., 2004), the observation site was relatively humid and warm condition compared to other Antarctic stations due to the effect of a marine environment. Values of the solar radiation varied between 2.3 W m^{-2} and 375.4 W m^{-2} , with a mean of $81.2 \pm 38.9\text{ W m}^{-2}$.

3.2 Seasonality in the physical characteristics of aerosol particles

3.2.1 Total particle number concentrations

Fig. 4 shows the monthly mean particle concentrations (CN) measured with two types of instruments (TSI CPC 3776 and 3772) over the period from March 2009 to February 2015. All the seasons mentioned in this study are austral seasons. As can be seen in Fig. 4, there is an evident seasonal cycle of CN concentrations, which are the maximum in the summer (DJF) and minimum in the winter (JJA). The maximum concentrations of particles larger than 2.5 nm ($\text{CN}_{2.5}$) and larger than 10 nm (CN_{10}) were approximately 2000 cm^{-3} in December 2012 and about 800 cm^{-3} in December 2009, respectively. The minimum values of $\text{CN}_{2.5}$ and CN_{10} concentrations were approximately 110 cm^{-3} and 90 cm^{-3} in August 2013, respectively. There are no significant anthropogenic sources of aerosol particles in Antarctica, therefore, our results were in good agreement with the results of previous studies from other Antarctic stations (Jaenicke et al., 1992; Gras, 1993; Virkkula et al., 2009; Weller et al., 2011). For instance, Virkkula et al. (2009) reported long-term daily average CN concentrations over the period from November 2003 to January 2007 from observations at Aboa, the Finnish Antarctic research station at a coastal region in Antarctica. The maximum monthly average CN concentrations were observed in February and the minimum concentrations were measured in July, which is the darkest



period of the year. The cause of the clear seasonal cycle of CN concentrations may be attributed to the formation process of aerosol particles. The major compounds of aerosol particles found at coastal Antarctic regions were non-sea-salt sulphate and methanesulphonate (MSA) derived from oxidation of dimethyl sulphide (DMS) produced by phytoplankton (Weller et al., 2011). The DMS concentrations increase sharply when biological activity is enhanced due to increasing temperatures and solar radiation (Virkkula et al., 2009). Since our sampling site was in the Antarctic Peninsula, ocean biological activity was considered to be an important factor in the particle formation and growth of aerosol particles. The CN concentrations typically increase in the summer due to high biological activity, while they decrease in the winter when biological activity is low. To better understand the effect of temperature and solar radiation intensity on CN_{2.5} concentrations, we compared the relationship between monthly mean CN_{2.5} concentrations and solar radiation intensity, and monthly mean CN_{2.5} concentrations and temperature. The correlation coefficient between CN_{2.5} and the solar radiation intensity (opened circle; R²=0.621) was higher than that between CN_{2.5} and temperature (opened triangle; R²=0.419), as shown in Fig. 5. Our results suggest that the CN_{2.5} concentrations may be more closely coupled with solar radiation intensity than with temperature.

A more detailed comparison of the monthly trends in the CN_{2.5} and CN₁₀ concentrations is presented in Fig. 6. The monthly mean CN concentrations increased from September to February mainly during the austral spring and summer periods. The CN concentrations sharply decreased from March and remained stable from April to August. In particular, the CN_{2.5} concentrations during the summer period increased sharply compared to the CN₁₀ concentrations, the increase was probably due to new particle formation. High solar radiation and temperature and low RH values during the summer are conducive to the new particle formation (Hamed et al., 2007).

3.2.2 Cloud condensation nuclei (CCN) concentrations

Fig. 7(a) shows the monthly mean CCN concentrations at the SS value of 0.4 % over the period from March 2009 to February 2015. There is a long gap in data from July 2011 to December 2013



because data were not collected due to a faulty CCN counter. We found monthly variations in the CCN concentrations with the maximum values being observed during the summer periods (DJF) and the minimum concentrations were observed during the winter periods (JJA). The monthly mean CCN concentrations were in the range of 20.63 cm^{-3} in July 2009 and 227.52 cm^{-3} in January 2014, with a mean of $112.80 \pm 39.05 \text{ cm}^{-3}$. It was similar to the seasonal cycle of the CN concentrations. Fig. 7(b) also shows seasonality in CCN concentrations at an SS value of 0.4 %. The CCN concentrations gradually decreased from February and remained stable during the winter, while the CCN concentrations from September increased sharply, as is shown in Fig. 7(b). The maximum CCN concentration in January was $199.89 \pm 37.07 \text{ cm}^{-3}$ and the minimum CCN concentration in August was $42.13 \pm 14.51 \text{ cm}^{-3}$. This clear seasonality of CCN concentrations is probably caused by the seasonal trend of CN concentrations. As shown in Fig. 6, CN_{10} concentrations as well as $\text{CN}_{2.5}$ concentrations increased during the summer. In addition, the aerosol size distributions measured by SMPS showed that concentrations of accumulation mode particles in the range of 100 and 300 nm as well as Aitken mode particles during the summer increased significantly, as can be seen in Fig. 8. Accumulation mode particles can easily act as CCN compared to nuclei or Aitken mode particles (Dusek et al., 2006), hence CCN concentrations increase during the summer and decrease during the winter.

In order to indirectly investigate the chemical characteristics of aerosol particles activated to CCN, the CCN spectra were examined in greater detail. An analysis of the cumulative CCN concentrations shown as a fraction of the CCN concentration measured at the SS of 1.0 % was carried out, and the results are shown in Fig. 9. Here, fractions of the CCN concentrations were estimated by dividing the CCN concentrations at each SS value by the total CCN concentrations at the SS of 1.0 %. Although a clear seasonal trend of CCN concentrations with a maximum during the summer and a minimum during the winter was presented, as mentioned earlier, the fraction of CCN concentrations at the SS value of 0.2 % in activated CCN concentrations showed a different pattern with a maximum value in July and a minimum value in December, as shown in Fig. 9. The numbers at the top of Fig. 9 represent



mean CCN concentrations at the SS values of 1.0 %. The fraction of particles activated to CCN at the SS value of 0.2 % during the summer and the winter was 0.49 ± 0.07 and 0.62 ± 0.06 , respectively. The fraction at the SS value of 0.2 % during the winter (JJA) was similar to those measured in Mace Head and Finokalia, which are regions representative of a marine environment (Paramonov et al., 2015). Our observations suggest that the major components in the aerosol particles that are activated to CCN at an SS of 0.2 % should be hygroscopic sea salts during the winter, while compounds less hygroscopic than sea salt would be dominant during the summer.

Fig. 10 illustrates the seasonal variations in the mean activation ratio of CCN concentrations at an SS of 0.4 % to the CN concentrations measured from two CPCs (TSI 3776 and 3772). The mean values of activation ratios of $\text{CCN}/\text{CN}_{2.5}$ and $\text{CCN}/\text{CN}_{10}$ were about 0.33 ± 0.10 and 0.40 ± 0.08 , respectively. Our results suggest that hygroscopic compounds were less dominant in the aerosol particles at our sampling site compared to levels in aerosol particles in the Arctic regions (Latham et al., 2013). Although clear changes were observed in the monthly variation in the CN and CCN concentrations as shown in Fig. 6 and Fig. 7(b), it was seen that the activation ratio ($\text{CCN}/\text{CN}_{10}$) was similar regardless of seasonality. The reason that no clear change is observed in the activation ratios at the King Sejong Station in the Antarctic Peninsula, might be the variation of the concentrations of accumulation mode particles, as can be seen in Fig. 8. The lower activation ratios in September and November are mainly because of the size and chemical properties of aerosol particles. Both, the size and chemical components of aerosol particles may have a large impact on the activation ratio (Dusek et al., 2006; Leena et al., 2016). The concentrations of Aitken mode aerosol particles increased sharply compared to their concentrations in August. Thus, the activation ratio decreased dramatically. Unfortunately, we did not confirm aerosol size distribution because our aerosol size distribution data in November was unreliable due to malfunctioning instruments.

The CCN concentrations at SS values can be represented by a power-law function, defined by Twomey (1959):



$$N_{CCN} = C \cdot (SS)^k \quad (1)$$

where N_{CCN} is the concentration of CCN at given a supersaturation values (SS), C and k are coefficient
5 constants estimated from CCN spectra. The values of C varied from 6.35 cm^{-3} to 837.24 cm^{-3} , with a
mean of $171.48 \pm 62.00 \text{ cm}^{-3}$. The values of k range between 0.07 and 2.19, with a mean of 0.41 ± 0.10 .
The monthly variations of k and C values are also summarized in Fig. 11. A comparison with CCN
concentrations indicated that the values of k during the austral winter (June) were also the lowest (0.29
 ± 0.06), while during the summer (December) they were the highest (0.55 ± 0.13). Based on this result,
10 aerosol particles activated to CCN during the summer are expected to be more sensitive to SS changes
than those during the winter.

3.2.3 Black carbon (BC) concentrations

Fig. 12 shows variations of monthly mean BC concentrations over the whole sampling periods. The
15 BC concentrations varied between 7.18 ng m^{-3} and 140.30 ng m^{-3} , with a mean of $64.68 \pm 12.17 \text{ ng m}^{-3}$.
The BC concentrations observed at our station were slightly higher than those at other stations in
Antarctica (Bodhaine, 1995; Wolff and Cachier, 1998; Pereira et al., 2006; Weller et al., 2013). For
instance, the annual mean BC concentrations at the South Pole, Halley, Neumayer, and Ferraz station
were 0.65, 1.0, 2.6, and 8.3 ng m^{-3} , respectively. Additionally, no clear seasonal patterns were observed
20 in our study throughout the entire observation period. However, clear seasonal patterns in previous
studies were observed at other stations in Antarctica (Wolff and Cachier, 1998; Weller et al., 2013).
Wolff and Cachier (1998) showed seasonal cycles of BC measured at the Hally station and South Pole
with a Aethalometer. They found that although BC concentrations varied depending on the sampling
site, the BC concentrations decreased during the austral winter (JJA) and increased during the austral
25 summer (DJF). Contrarily, according to Pereira et al. (2006), although BC concentration during the
summer increased slightly, no clear seasonal trends were observed unlike the results measured by Wolff



and Cachier (1998). This suggests that the BC concentrations are dependent on the sampling site and the long-range transport of air masses.

3.3 Effect of air mass trajectory on the physical properties of aerosol particles

5 In this section, the effect of the origin and pathway of air mass on the physical characteristic of aerosol particles is presented. As mentioned earlier in Sec. 2.3, we classified air masses into four groups based on air mass back trajectory analysis. The wind data and aerosol characteristics with the four types of air masses during the entire observation period are listed in Table 1. Although they are unreliable due to the low observation frequency compared to the other types of air masses, as shown
10 in Table 1, the BC and CCN concentrations were the highest when the air mass originated from the continent of South America (Case 1). This might be due to anthropogenic influences at the source and the aging of aerosol particles. The CN_{10} concentrations were similar regardless of the origin and pathway of air masses, whereas an enhancement of the $CN_{2.5}$ concentrations was observed when the air mass originated from the ocean (Case 2 and 4). This is probably due to the high biological activity
15 in the South Atlantic and South Pacific Oceans during the summer (DJF) period. A more detailed comparison, excluding the results of Case 1 of the CN concentrations based on the air mass analysis is shown in Fig. 13. Minimum concentrations of aerosol particles ($CN_{2.5}$ and CN_{10}) originating from the ocean (Case 2 and 4) were observed from April to September, whereas concentrations of aerosol particles ($CN_{2.5}$) originating from the South Atlantic (Case 2) and the South Pacific (Case 4) Oceans
20 were the highest in November and February, respectively. Here we found that the peak month of the $CN_{2.5}$ concentrations had discrepancies in accordance with the air mass history. This is probably due to difference in chemical compounds that contributed to aerosol formation processes and/or in variations of biogenic activity according to the origin and transport pathway of air masses. To verify this, further studies on chemical compositions of aerosol particles need to be carried out in the future.

25 When air masses were transported from the South Pacific Ocean to the King Sejong Station (Case 4), the seasonality of aerosol size distribution was also investigated. The lognormal fitted aerosol size



distribution ranged from 0.01 to 0.3 μm is presented in Fig. 14. The modal diameters with standard deviation and number concentrations are summarized in Table 2. It is obvious that the modal diameters during the summer are larger than those during the winter for, both Aitken and accumulation modes: 0.023 μm in the winter and 0.034 μm in the summer for the Aitken mode and 0.086 μm in the winter and 0.109 μm in the summer for the accumulation mode. The number concentrations for the summer are also higher than the value for the winter for the Aitken and accumulation modes, $49.16 \pm 3.88 \text{ cm}^{-3}$ during the winter and $304.36 \pm 20.10 \text{ cm}^{-3}$ during the summer for the Aitken mode and $44.78 \pm 14.24 \text{ cm}^{-3}$ in the winter and $140.25 \pm 10.64 \text{ cm}^{-3}$ in the summer for the accumulation mode. The enhancement of number concentrations for the Aitken mode during the summer should be linked to new particle formation over oceans as a product of biological activity. The spring and autumn seasons show intermediate values. Our results are similar those of previous laboratory and field experiments (Sellegri et al., 2006; Yoon et al., 2007). O'Dowd et al. (2004) suggested that primary formation processes play a significant role in marine aerosol production in the North Atlantic Ocean. In addition, the contribution of biological organic compounds to the marine aerosol distribution might be dominant (Kim et al., 2015).

4 Summary and conclusions

The seasonal variations in the physical characteristics of aerosol particles at the King Sejong Station (62.22°S, 58.78°W) in the Antarctic Peninsula were investigated based on the in-situ measured aerosol data for the period from March 2009 to February 2015. An obvious seasonal variation of particle number concentrations (CN) exists, with the maximum concentrations in the austral summer (DJF) and the minimum concentrations in the winter (JJA). The maximum CN concentrations of particles larger than 2.5 nm ($\text{CN}_{2.5}$) and 10 nm (CN_{10}) were approximately 2000 cm^{-3} in December 2012 and about 800 cm^{-3} in December 2009 and February 2015, respectively. In particular, $\text{CN}_{2.5}$ concentrations increased sharply during the summer compared to CN_{10} concentrations, suggesting that the particle formation processes were probably driven by the high biological activity during the season.



In addition, we presented the seasonality of CCN. The maximum mean CCN concentration of $199.89 \pm 37.07 \text{ cm}^{-3}$ was measured in January and the minimum mean CCN concentration was $42.13 \pm 14.51 \text{ cm}^{-3}$ in August. The activation ratio ($\text{CCN}/\text{CN}_{10}$) of aerosol particles at the King Sejong Station (0.40 ± 0.08) in the Antarctic Peninsula was lower than those at the Arctic sites (0.52), indicating that less hygroscopic compounds in aerosol particles should be dominant. We also estimated C and k values from measured CCN results at certain SS values. The values of C varied between 6.35 cm^{-3} and 837.24 cm^{-3} , with a mean of $171.48 \pm 62.00 \text{ cm}^{-3}$. The values of k ranged between 0.07 and 2.19, with a mean of 0.41 ± 0.10 . The k values during austral the summer periods (DJF) were higher than those during the winter periods (JJA).

Based on the backward trajectory analysis, we classified the air mass into four groups according to their origin and pathway: two continental regions (South America and Antarctica) and two oceanic areas (South Atlantic and South Pacific Ocean). We found that most air masses originated from the oceanic areas. Although the BC and CCN concentrations were the highest when the air mass originated from the South American continent, the results are not significant because only a small amount of data was analyzed. The CN_{10} concentrations were analogous regardless of origin, whereas $\text{CN}_{2.5}$ concentrations showed differing values. The $\text{CN}_{2.5}$ concentrations that originated from oceanic areas (Case 2 and 4) were higher than those from continental regions (Case 3), in particular, the $\text{CN}_{2.5}$ concentrations show clear seasonal variations; minimum concentrations from April to September and maximum concentrations in November from the South Atlantic Ocean (Case 2) and in February from the South Pacific Ocean (Case 4). Furthermore, in terms of Case 4, an analysis of aerosol size distributions in the 0.01-0.3 μm range was performed. The modal diameters also showed seasonal variations, 0.023 μm in the winter and 0.034 μm in the summer for the Aitken mode and 0.086 μm in the winter and 0.109 μm in the summer for the accumulation mode.

Overall, this study is the first of its kind to analyze seasonal variations in the physical characteristics of aerosol particles in the Antarctic Peninsula. The aerosol particle formation process is still not fully



understood, and thus, more studies should be necessary to determine seasonal variations in the chemical characteristics of atmospheric aerosols.

Acknowledgements

- 5 We would like to thank the many technicians and scientists of the overwintering crews. This work was supported by a Korea Grant from the Korean Government (MSIP) (NRF-2016M1A5A1901769) (KOPRI-PN16081) and the KOPRI project (PE16010).

References

- 10 Arimoto, R., Hogan, A., Grube, P., Davis, D., Webb, J., Schloesslin, C., Sage, S., and Raccach, F.: Major ions and radionuclides in aerosol particles from the South Pole during ISCAT-2000, *Atmos. Environ.*, 38, 5473-5484, 10.1016/j.atmosenv.2004.01.049, 2004.
- Asmi, E., Frey, A., Virkkula, A., Ehn, M., Manninen, H. E., Timonen, H., Tolonen-Kiviäki, O., Aurela, M., Hillamo, R., and Kulmala, M.: Hygroscopicity and chemical composition of antarctic sub-micrometre aerosol particles and observations of new particle formation, *Atmos. Chem. Phys.*, 15, 4253-4271, 10.5194/acp-10-4253-2010, 2010.
- Belosi, F., Contini, D., Donato, A., Santachiara, G., and Prodi, F.: Aerosol size distribution at Nansen Ice Sheet Antarctica, *Atmos. Res.*, 107, 42-50, 10.1016/j.atmosres.2011.12.007, 2012.
- Bodhaine, B. A.: Aerosol absorption measurements at Barrow, Mauna Loa and the south pole, *J. Geophys. Res.*, 100, 8967-8975, 10.1029/95jd00513, 1995.
- 20 Chen, J. L., Wilson, C. R., Blankenship, D., and Tapley, B. D.: Accelerated Antarctic ice loss from satellite gravity measurements, *Nat. Geosci.*, 2, 859-862, 10.1038/ngeo694, 2009.
- Choi, T., Lee, B. Y., Kim, S. J., Yoon, Y. J., and Lee, H. C.: Net radiation and turbulent energy exchanges over a non-glaciated coastal area on King George Island during four summer seasons, *Antarct. Sci.*, 20, 99-111, 10.1017/s095410200700082x, 2008.
- 25 Dusek, U., Frank, G. P., Hildebrandt, L., Curtius, J., Schneider, J., Walter, S., Chand, D., Drewnick, F., Hings, S., Jung, D., Borrmann, S., and Andreae, M. O.: Size matters more than chemistry for cloud-nucleating ability of aerosol particles, *Science*, 312, 1375-1378, 10.1126/science.1125261, 2006.
- 30 Fiebig, M., Hirdman, D., Lunder, C. R., Ogren, J. A., Solberg, S., Stohl, A., and Thompson, R. L.: Annual cycle of Antarctic baseline aerosol: Controlled by photooxidation-limited aerosol



- formation, *Atmos. Chem. Phys.*, 14, 3083-3093, 10.5194/acp-14-3083-2014, 2014.
- Gras, J. L.: Condensation nucleus size distribution at Mawson, Antarctica: Microphysics and chemistry, *Atmos. Environ.*, 27A, 1427-1434, 10.1016/0960-1686(93)90128-1, 1993.
- Hamed, A., Joutsensaari, J., Mikkonen, S., Sogacheva, L., Dal Maso, M., Kulmala, M., Cavalli, F.,
5 Fuzzi, S., Facchini, M. C., Decesari, S., Mircea, M., Lehtinen, K. E. J., and Laaksonen, A.:
Nucleation and growth of new particles in Po Valley, Italy, *Atmos. Chem. Phys.*, 7, 355-376, 2007.
- Hansen, A. D. A., Lowenthal, D. H., Chow, J. C., and Watson, J. G.: Black carbon aerosol at McMurdo
Station, Antarctica, *J. Air Waste Manage. Assoc.*, 51, 593-600, 2001.
- Hara, K., Hirasawa, N., Yamanouchi, T., Wada, M., and Herber, A.: Spatial distributions and mixing
10 states of aerosol particles in the summer Antarctic troposphere, *Antarctic Record*, 54, 704-730,
2010.
- Hara, K., Osada, K., Nishita-Hara, C., Yabuki, M., Hayashi, M., Yamanouchi, T., Wada, M., and
Shiobara, M.: Seasonal features of ultrafine particle volatility in the coastal Antarctic troposphere,
Atmos. Chem. Phys., 11, 9803-9812, 10.5194/acp-11-9803-2011, 2011a.
- 15 Hara, K., Osada, K., Nishita-Hara, C., and Yamanouchi, T.: Seasonal variations and vertical features
of aerosol particles in the Antarctic troposphere, *Atmos. Chem. Phys.*, 11, 5471-5484,
10.5194/acp-11-5471-2011, 2011b.
- IPCC: Climate change 2013: The physical science basis, Intergovernmental panel on Climate Change,
Cambridge University Press, New York, USA, 571-740, 2013.
- 20 Ito, T.: Study of background aerosols in the Antarctic troposphere, *J. Atmos. Chem.*, 3, 69-91,
10.1007/bf00049369, 1985.
- Jaenicke, R., Dreiling, V., Lehmann, E., Koutsenogui, P. K., and Stingl, J.: Condensation nuclei at the
German Antarctic Station "Georg von Neumayer", *Tellus Ser. B*, 44 B, 311-317, 1992.
- Järvinen, E., Virkkula, A., Nieminen, T., Aalto, P. P., Asmi, E., Lanconelli, C., Busetto, M., Lupi, A.,
25 Schioppo, R., Vitale, V., Mazzola, M., Petäjä, T., Kerminen, V. M., and Kulmala, M.: Seasonal
cycle and modal structure of particle number size distribution at Dome C, Antarctica, *Atmos.
Chem. Phys.*, 13, 7473-7487, 10.5194/acp-13-7473-2013, 2013.
- Kim, G., Cho, H. J., Seo, A., Kim, D., Gim, Y., Lee, B. Y., Yoon, Y. J., and Park, K.: Comparison of
Hygroscopicity, Volatility, and Mixing State of Submicrometer Particles between Cruises over the
30 Arctic Ocean and the Pacific Ocean, *Environ. Sci. Technol.*, 49, 12024-12035,
10.1021/acs.est.5b01505, 2015.
- Koponen, I. K., Virkkula, A., Hillamo, R., Kerminen, V. M., and Kulmala, M.: Number size
distributions and concentrations of the continental summer aerosols in Queen Maud Land,
Antarctica, *J. Geophys. Res. D: Atmos.*, 108, AAC 8-1 - AAC 8-10, 2003.



- Kwon, T. Y., and Lee, B. Y.: Precipitation anomalies around King Sejong Station, Antarctica associated with El Niño/Southern Oscillation, *Ocean and Polar Research*, 24, 19-31, 2002.
- Kyrö, E. M., Kerminen, V. M., Virkkula, A., Dal Maso, M., Parshintsev, J., Ruíz-Jimenez, J., Forsström, L., Manninen, H. E., Riekkola, M. L., Heinonen, P., and Kulmala, M.: Antarctic new particle formation from continental biogenic precursors, *Atmos. Chem. Phys.*, 13, 3527-3546, 10.5194/acp-13-3527-2013, 2013.
- Latham, T. L., Beyersdorf, A. J., Thornhill, K. L., Winstead, E. L., Cubison, M. J., Hecobian, A., Jimenez, J. L., Weber, R. J., Anderson, B. E., and Nenes, A.: Analysis of CCN activity of Arctic aerosol and Canadian biomass burning during summer 2008, *Atmos. Chem. Phys.*, 13, 2735-2756, 10.5194/acp-13-2735-2013, 2013.
- Leena, P. P., Pandithurai, G., Anilkumar, V., Murugavel, P., Sonbawne, S. M., and Dani, K. K.: Seasonal variability in aerosol, CCN and their relationship observed at a high altitude site in Western Ghats, *Meteorology and Atmospheric Physics*, 128, 143-153, 10.1007/s00703-015-0406-0, 2016.
- Mazzer, D. M., Lowenthal, D. H., Chow, J. C., and Watson, J. G.: Sources of PM₁₀ and sulfate aerosol at McMurdo station, Antarctica, *Chemosphere*, 45, 347-356, 10.1016/s0045-6535(00)00591-9, 2001.
- Mishra, V. K., Kim, K. H., Hong, S., and Lee, K.: Aerosol composition and its sources at the King Sejong Station, Antarctic peninsula, *Atmos. Environ.*, 38, 4069-4084, 10.1016/j.atmosenv.2004.03.052, 2004.
- O'Dowd, C. D., Facchini, M. C., Cavalli, F., Ceburnis, D., Mircea, M., Decesari, S., Fuzzi, S., Young, J. Y., and Putaud, J. P.: Biogenically driven organic contribution to marine aerosol, *Nature*, 431, 676-680, 10.1038/nature02959, 2004.
- Pant, V., Siingh, D., and Kamra, A. K.: Size distribution of atmospheric aerosols at Maitri, Antarctica, *Atmos. Environ.*, 45, 5138-5149, 2011.
- Paramonov, M., Kerminen, V. M., Gysel, M., Aalto, P. P., Andreae, M. O., Asmi, E., Baltensperger, U., Bougiatioti, A., Brus, D., Frank, G. P., Good, N., Gunthe, S. S., Hao, L., Irwin, M., Jaatinen, A., Jurányi, Z., King, S. M., Kortelainen, A., Kristensson, A., Lihavainen, H., Kulmala, M., Lohmann, U., Martin, S. T., McFiggans, G., Mihalopoulos, N., Nenes, A., O'Dowd, C. D., Ovadnevaite, J., Petäjä, T., Pöschl, U., Roberts, G. C., Rose, D., Svenningsson, B., Swietlicki, E., Weingartner, E., Whitehead, J., Wiedensohler, A., Wittbom, C., and Sierau, B.: A synthesis of cloud condensation nuclei counter (CCNC) measurements within the EUCAARI network, *Atmos. Chem. Phys.*, 15, 12211-12229, 10.5194/acp-15-12211-2015, 2015.
- Park, J., Sakurai, H., Vollmers, K., and McMurry, P. H.: Aerosol size distributions measured at the



- South Pole during ISCAT, *Atmos. Environ.*, 38, 5493-5500, 10.1016/j.atmosenv.2002.12.001, 2004.
- Pereira, E. B., Evangelista, H., Pereira, K. C. D., Cavalcanti, I. F. A., and Setzer, A. W.: Apportionment of black carbon in the South Shetland Islands, Antarctic Peninsula, *J. Geophys. Res.: Atmos.*, 111, 10.1029/2005jd006086, 2006.
- 5 Pritchard, H. D., Ligtenberg, S. R. M., Fricker, H. A., Vaughan, D. G., Van Den Broeke, M. R., and Padman, L.: Antarctic ice-sheet loss driven by basal melting of ice shelves, *Nature*, 484, 502-505, 10.1038/nature10968, 2012.
- Rankin, A. M., and Wolff, E. W.: A year-long record of size-segregated aerosol composition at Halley, Antarctica, *J. Geophys. Res. D: Atmos.*, 108, AAC 9-1 - AAC 9-12, 2003.
- 10 Rignot, E., Casassa, G., Gogineni, P., Krabill, W., Rivera, A., and Thomas, R.: Accelerated ice discharge from the Antarctic Peninsula following the collapse of Larsen B ice shelf, *Geophys. Res. Lett.*, 31, L18401 18401-18404, 10.1029/2004gl020697, 2004.
- Roscoe, H. K., Jones, A. E., Brough, N., Weller, R., Saiz-Lopez, A., Mahajan, A. S., Schoenhardt, A., Burrows, J. P., and Fleming, Z. L.: Particles and iodine compounds in coastal Antarctica, *J. Geophys. Res. D: Atmos.*, 120, 7144-7156, 10.1002/2015jd023301, 2015.
- 15 Schneider, D. P., Deser, C., and Okumura, Y.: An assessment and interpretation of the observed warming of West Antarctica in the austral spring, *Clim. Dyn.*, 38, 323-347, 10.1007/s00382-010-0985-x, 2012.
- 20 Sellegri, K., O'Dowd, C. D., Yoon, Y. J., Jennings, S. G., and de Leeuw, G.: Surfactants and submicron sea spray generation, *J. Geophys. Res.: Atmos.*, 111, 10.1029/2005jd006658, 2006.
- Shaw, G. E.: Optical, chemical and physical properties of aerosols over the antarctic ice sheet, *Atmos. Environ.*, 14, 911-921, 10.1016/0004-6981(80)90004-9, 1980.
- Steig, E. J., Schneider, D. P., Rutherford, S. D., Mann, M. E., Comiso, J. C., and Shindell, D. T.: Warming of the Antarctic ice-sheet surface since the 1957 International Geophysical Year, *Nature*, 25 457, 459-462, 10.1038/nature07669, 2009.
- Stein, A. F., Draxler, R. R., Rolph, G. D., Stunder, B. J. B., Cohen, M. D., and Ngan, F.: NOAA's hysplit atmospheric transport and dispersion modeling system, *Bull. Amer. Meteorol. Soc.*, 96, 2059-2077, 10.1175/bams-d-14-00110.1, 2015.
- 30 Tomasi, C., Vitale, V., Lupi, A., Di Carmine, C., Campanelli, M., Herber, A., Treffeisen, R., Stone, R. S., Andrews, E., Sharma, S., Radionov, V., von Hoyningen-Huene, W., Stebel, K., Hansen, G. H., Myhre, C. L., Wehrli, C., Aaltonen, V., Lihavainen, H., Virkkula, A., Hillamo, R., Ström, J., Toledano, C., Cachorro, V. E., Ortiz, P., de Frutos, A. M., Blindheim, S., Frioud, M., Gausa, M., Zielinski, T., Petelski, T., and Yamanouchi, T.: Aerosols in polar regions: A historical overview



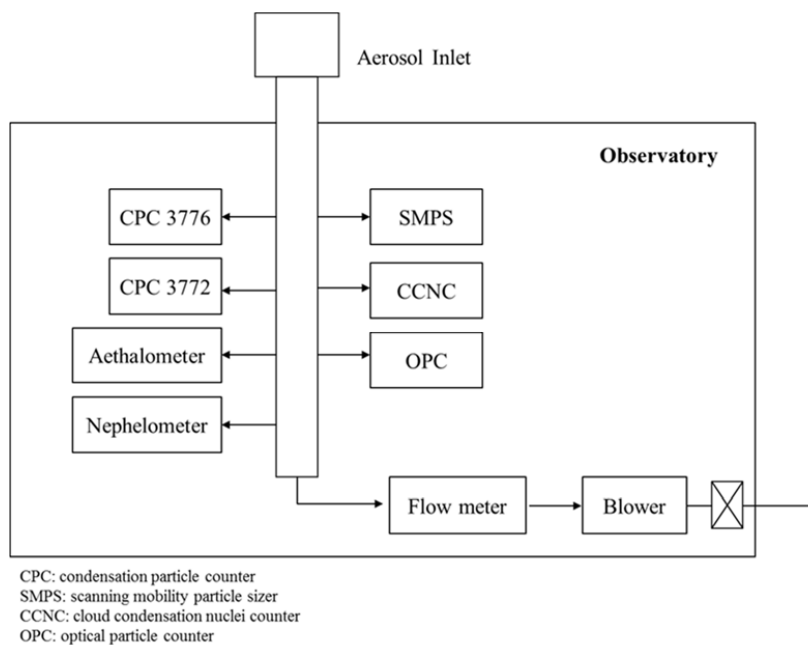
- based on optical depth and in situ observations, *J. Geophys. Res.: Atmos.*, 112, 10.1029/2007jd008432, 2007.
- Tunved, P., Ström, J., and Krejci, R.: Arctic aerosol life cycle: Linking aerosol size distributions observed between 2000 and 2010 with air mass transport and precipitation at Zeppelin station, Ny-Ålesund, Svalbard, *Atmos. Chem. Phys.*, 13, 3643-3660, 10.5194/acp-13-3643-2013, 2013.
- Twomey, S.: The nuclei of natural cloud formation part II: The supersaturation in natural clouds and the variation of cloud droplet concentration, *Geophys. Pura Appl.*, 43, 243-249, 10.1007/bf01993560, 1959.
- Vaughan, D. G., Marshall, G. J., Connolley, W. M., Parkinson, C., Mulvaney, R., Hodgson, D. A., King, J. C., Pudsey, C. J., and Turner, J.: Recent rapid regional climate warming on the Antarctic Peninsula, *Clim. Change*, 60, 243-274, 10.1023/a:1026021217991, 2003.
- Virkkula, A., Teinilä, K., Hillamo, R., Kerminen, V. M., Saarikoski, S., Aurela, M., Koponen, I. K., and Kulmala, M.: Chemical size distributions of boundary layer aerosol over the Atlantic Ocean and at an Antarctic site, *J. Geophys. Res.: Atmos.*, 111, 10.1029/2004jd004958, 2006.
- Virkkula, A., Hirsikko, A., Vana, M., Aalto, P. P., Hillamo, R., and Kulmala, M.: Charged particle size distributions and analysis of particle formation events at the Finnish Antarctic research station Aboa, *Boreal Environ. Res.*, 12, 397-408, 2007.
- Virkkula, A., Asmi, E., Teinilä, K., Frey, A., Aurela, M., Timonen, H., Mäkelä, T., Samuli, A., Hillamo, R., Aalto, P. P., Kirkwood, S., and Kulmala, M.: Review of aerosol research at the Finnish Antarctic research station Aboa and its surroundings in Queen Maud Land, Antarctica, *Geophysica*, 45, 163-181, 2009.
- Weller, R., and Wagenbach, D.: Year-round chemical aerosol records in continental Antarctica obtained by automatic samplings, *Tellus Ser. B-Chem. Phys. Meteorol.*, 59, 755-765, 10.1111/j.1600-0889.2007.00293.x, 2007.
- Weller, R., and Lampert, A.: Optical properties and sulfate scattering efficiency of boundary layer aerosol at coastal Neumayer Station, Antarctica, *J. Geophys. Res.: Atmos.*, 113, 10.1029/2008jd009962, 2008.
- Weller, R., Minikin, A., Wagenbach, D., and Dreiling, V.: Characterization of the inter-annual, seasonal, and diurnal variations of condensation particle concentrations at Neumayer, Antarctica, *Atmos. Chem. Phys.*, 11, 13243-13257, 10.5194/acp-11-13243-2011, 2011.
- Weller, R., Minikin, A., Petzold, A., Wagenbach, D., and König-Langlo, G.: Characterization of long-term and seasonal variations of black carbon (BC) concentrations at Neumayer, Antarctica, *Atmos. Chem. Phys.*, 13, 1579-1590, 10.5194/acp-13-1579-2013, 2013.
- Weller, R., Schmidt, K., Teinilä, K., and Hillamo, R.: Natural new particle formation at the coastal



Antarctic site Neumayer, Atmos. Chem. Phys., 15, 11399-11410, 10.5194/acp-15-11399-2015, 2015.

Wolff, E. W., and Cachier, H.: Concentrations and seasonal cycle of black carbon in aerosol at a coastal Antarctic station, J. Geophys. Res. D: Atmos., 103, 11033-11041, 1998.

- 5 Yoon, Y. J., Ceburnis, D., Cavalli, F., Jourdan, O., Putaud, J. P., Facchini, M. C., Decesari, S., Fuzzi, S., Sellegri, K., Jennings, S. G., and O'Dowd, C. D.: Seasonal characteristics of the physicochemical properties of North Atlantic marine atmospheric aerosols, J. Geophys. Res.: Atmos., 112, 10.1029/2005jd007044, 2007.



5 Figure 1. A schematic diagram for the observation methods used in this study.

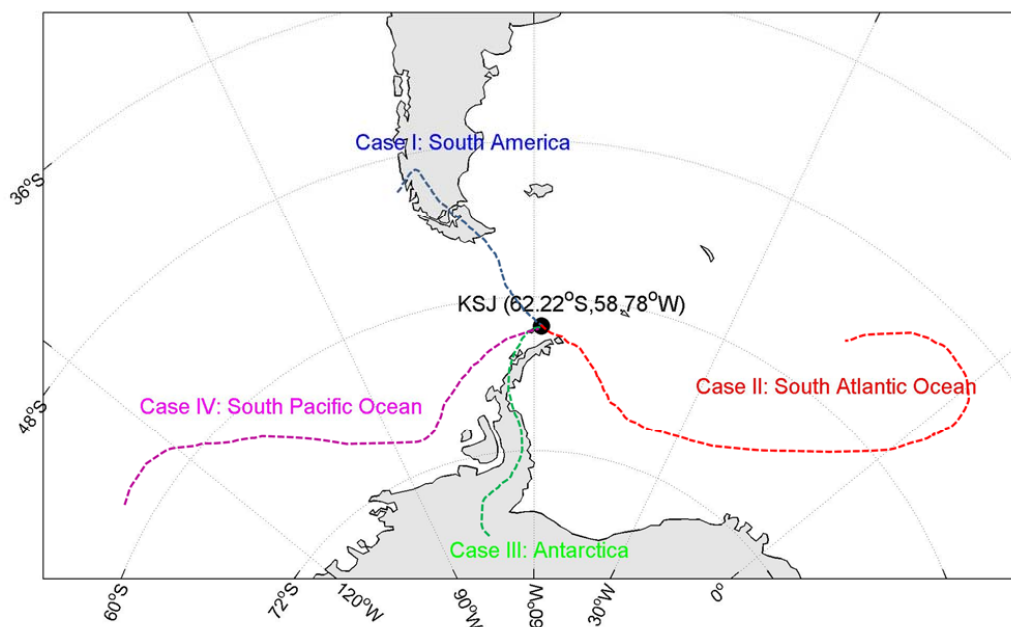


Figure 2. Map of the sampling site (62.22°S, 58.78°W; black circle) and classification of the four cases
5 according to the origin and pathway of the air masses. Dot lines represent example of back trajectories according to cases.

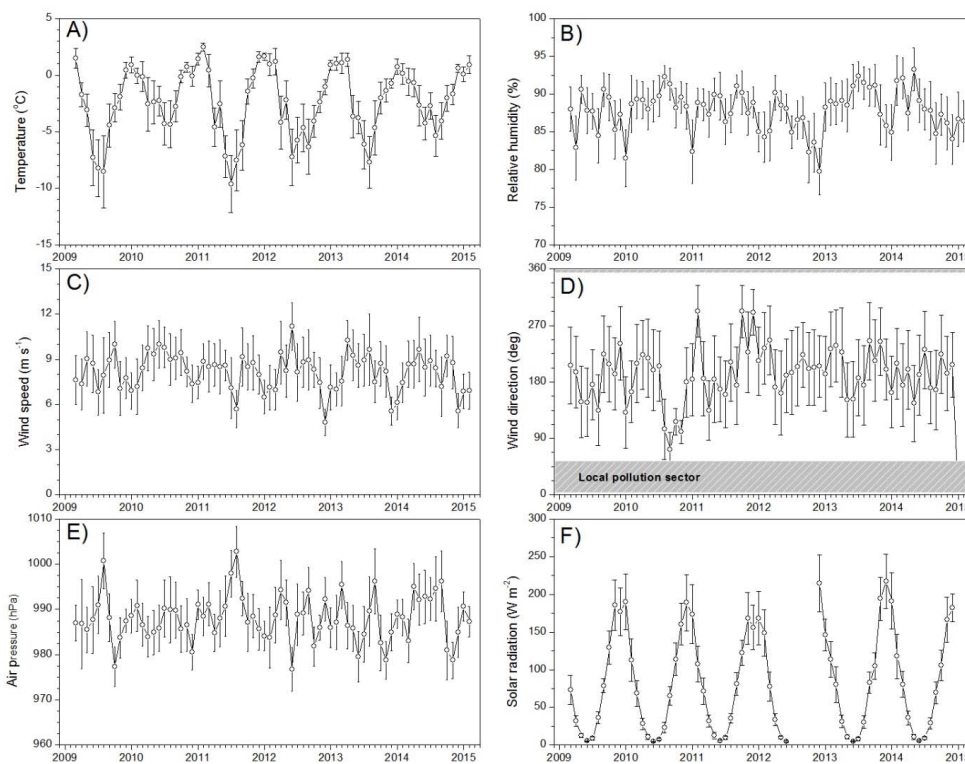


Figure 3. Monthly mean variation of (a) temperature, (b) relative humidity, (c) wind speed, (d) wind
5 direction, (e) air pressure, and (f) solar radiation over the period from March 2009 to February 2015.
The shaded area in Figure 3(d) represents the wind direction for the local pollution sector.

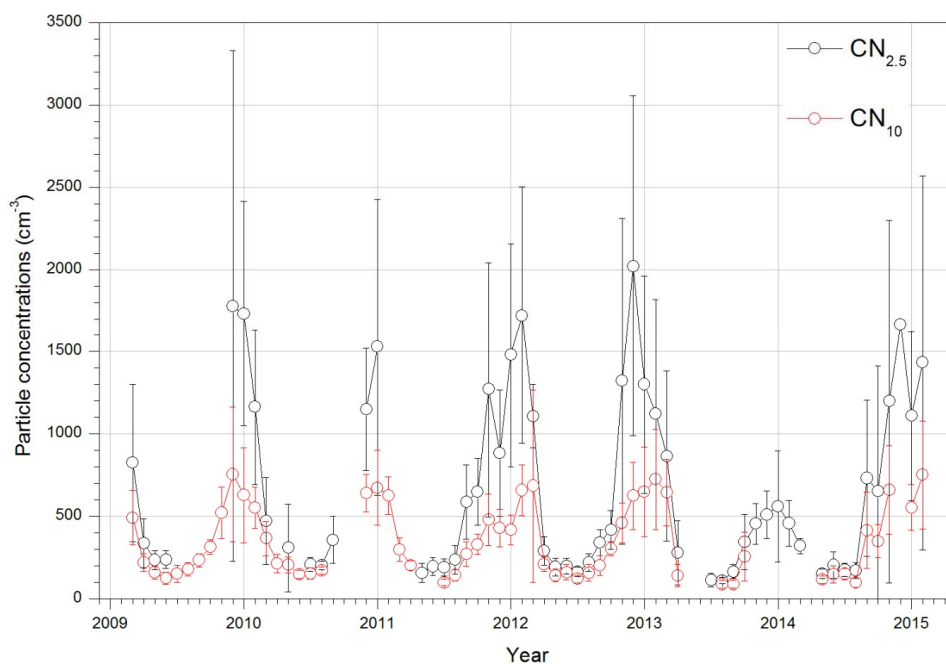


Figure 4. Monthly variations of mean $\text{CN}_{2.5}$ (black opened circle) and CN_{10} (red opened circle) concentrations with a standard deviation from March 2009 to February 2015.

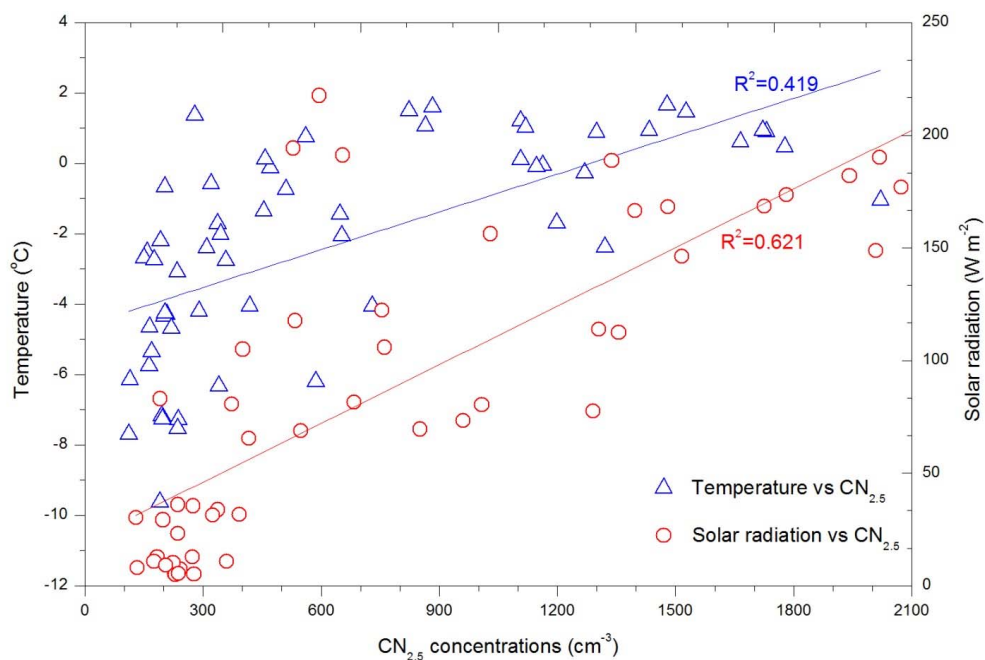


Figure 5. Scatterplot diagram of monthly mean CN_{2.5} concentrations and monthly mean temperature (blue opened triangle) or monthly mean solar radiation intensity (red opened circle). Blue and red solid lines are a regression lines.
5

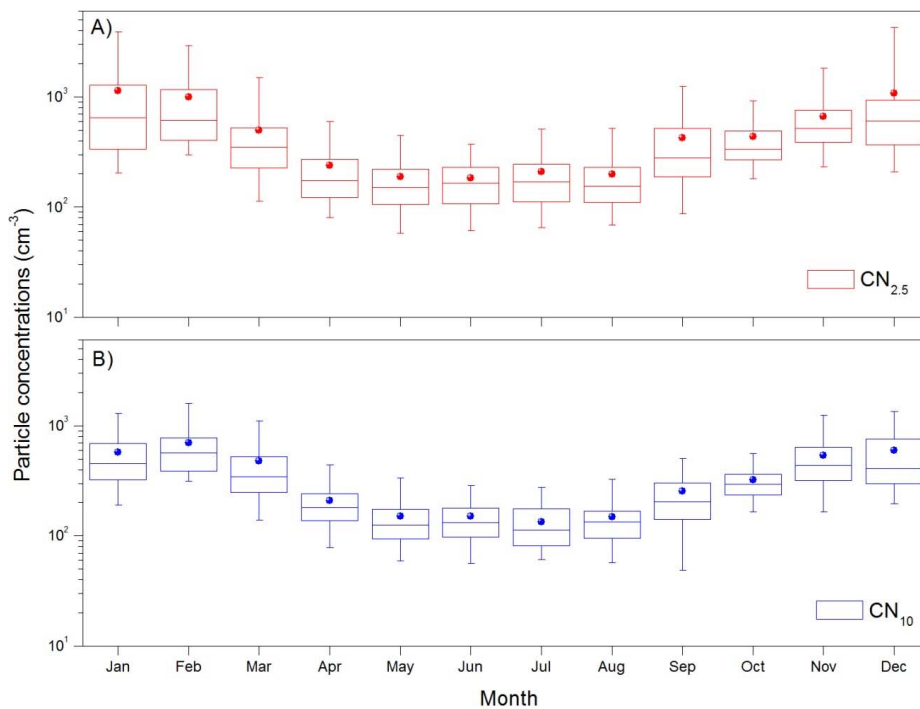


Figure 6. Box plots of seasonality of (a) CN_{2.5} and (b) CN₁₀ concentrations. Lines in the middle of the boxes indicate sample medians (mean: circle), lower and upper lines of the boxes are the 25th and 75th percentiles, and whiskers indicate the 5th and 95th percentiles.

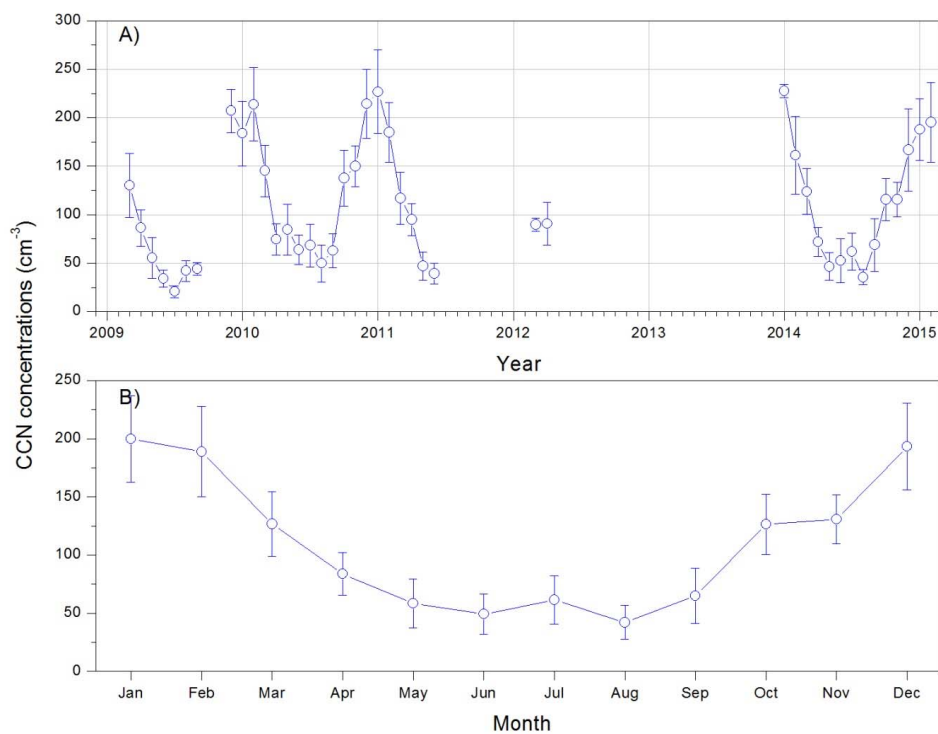


Figure 7. (a) Monthly mean CCN concentrations at the SS of 0.4 % with a standard deviation from March 2009 to February 2015 (b) Seasonal variation of mean CCN concentrations at the SS of 0.4 % with a standard deviation.

5

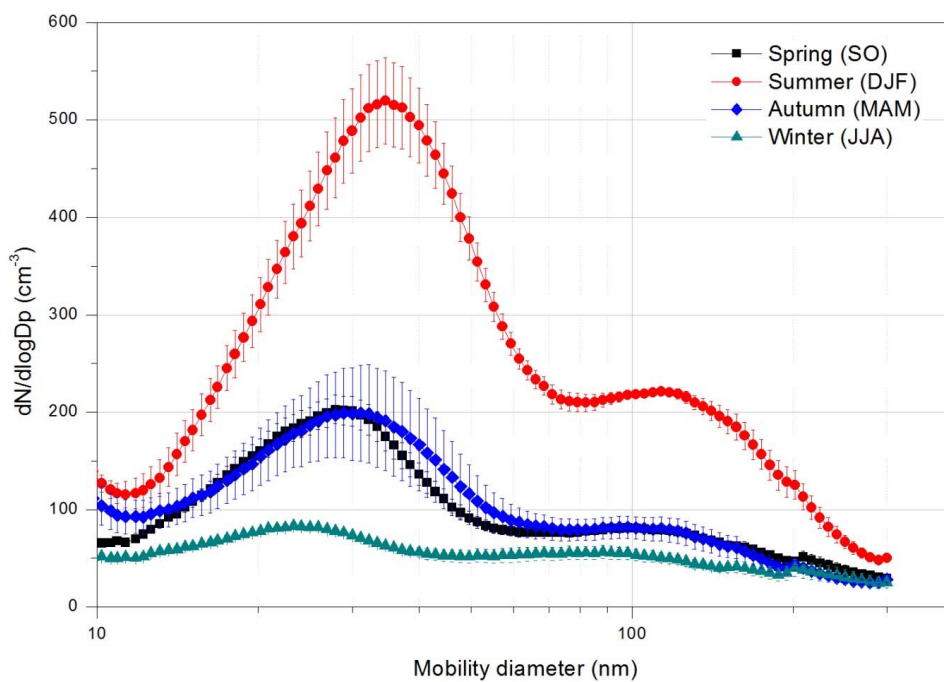


Figure 8. Seasonal mean aerosol size distribution measured by the SMPS at the King Sejong research station over the period from March 2009 to February 2015.

5

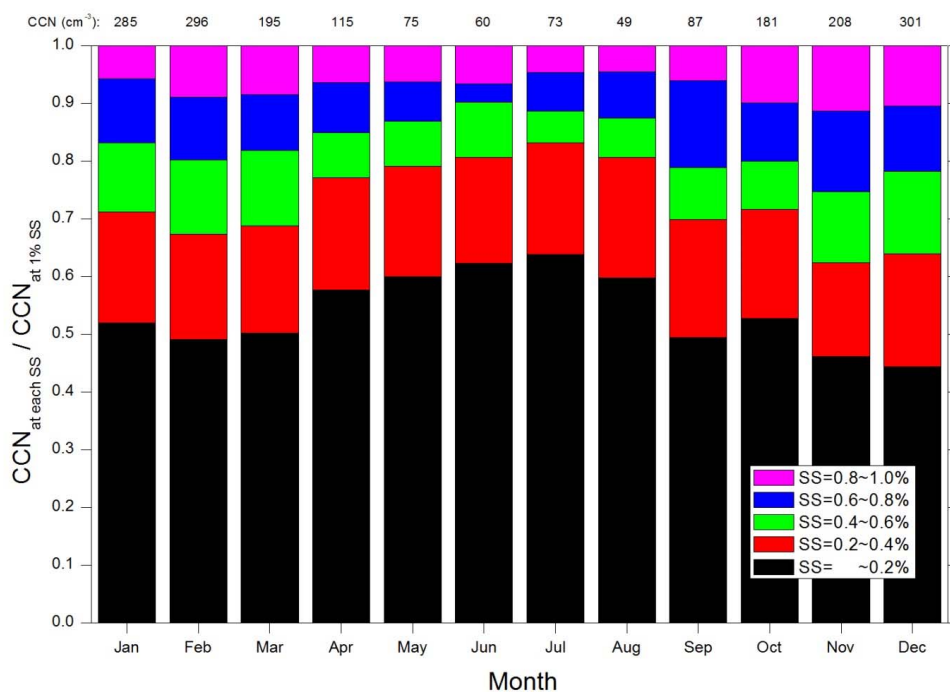


Figure 9. Monthly mean cumulative CCN concentrations shown as fractions of the CCN concentration at the SS of 1.0 %. Colours indicate the SS bins. The number at top of figure represents monthly mean
5 CCN concentrations at the SS values of 1.0 %.

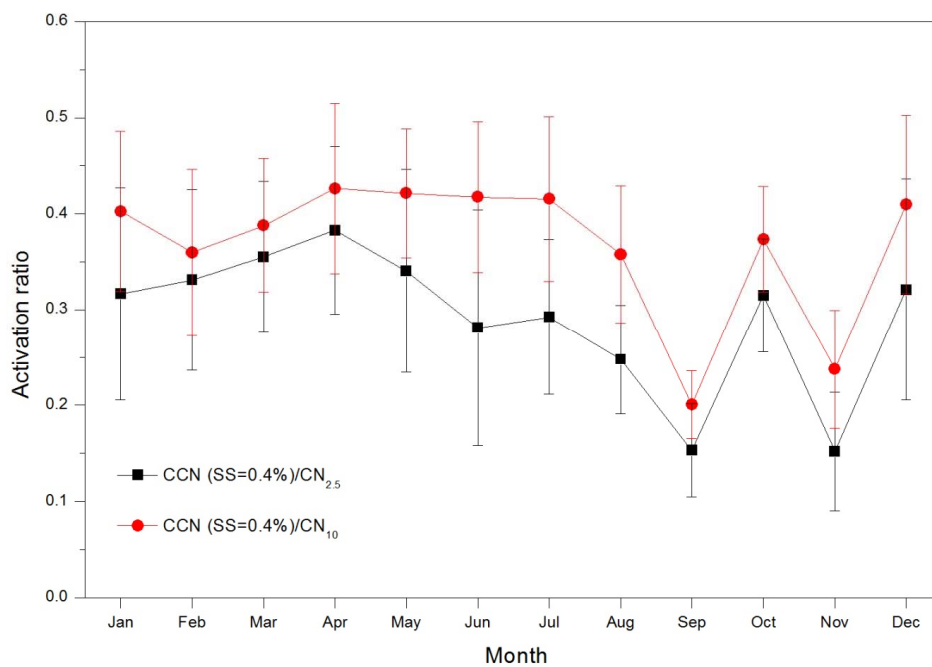


Figure 10. Comparison of the seasonal mean variation of the activation ratio between measurements
5 (CPC 3776 and CPC 3772) by two CPCs.

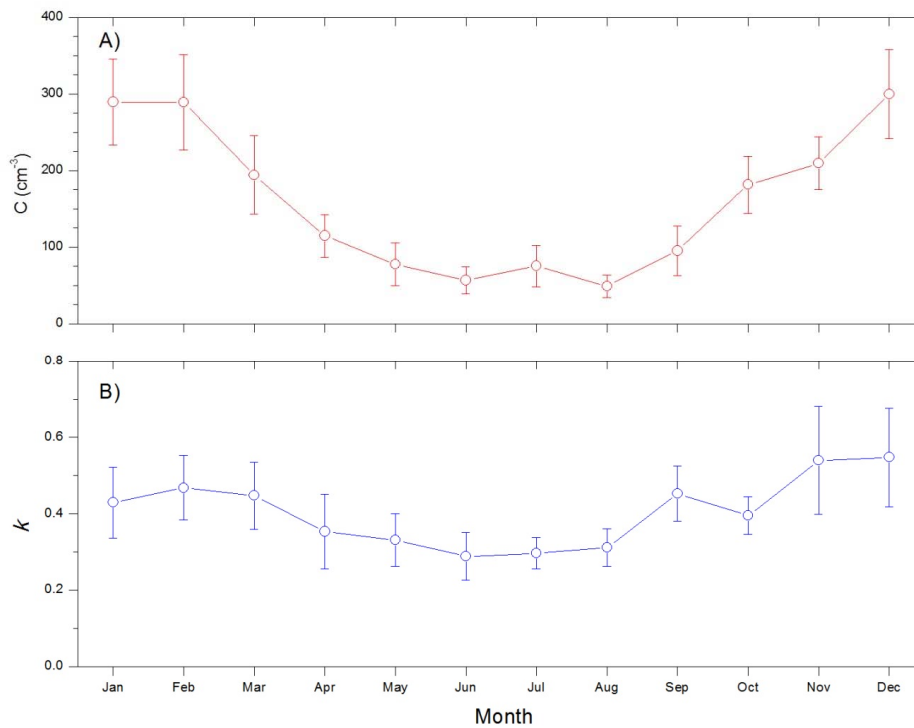


Figure 11. Seasonality of monthly mean values of (a) C and (b) k over the whole observation periods.

5

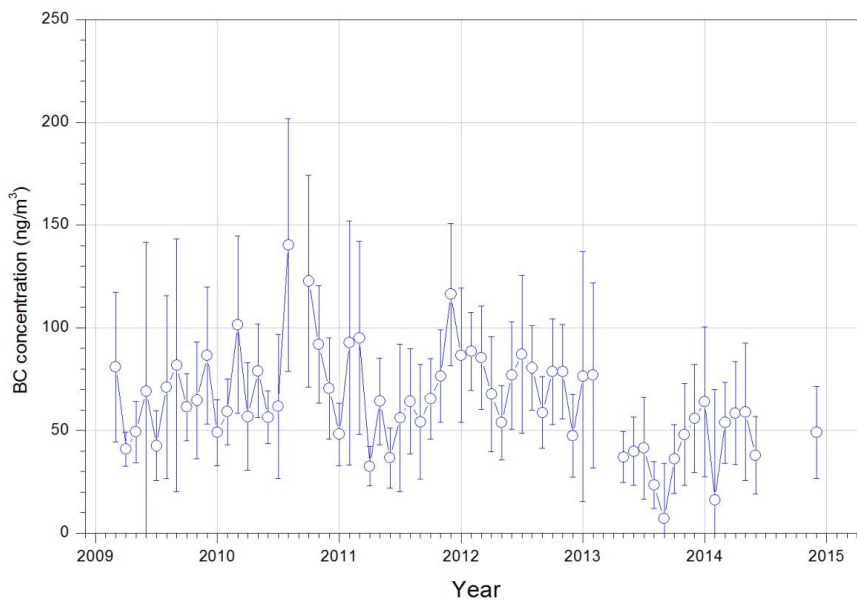


Figure 12. Monthly mean concentrations of black carbon over the period from March 2009 to February 2015.

5

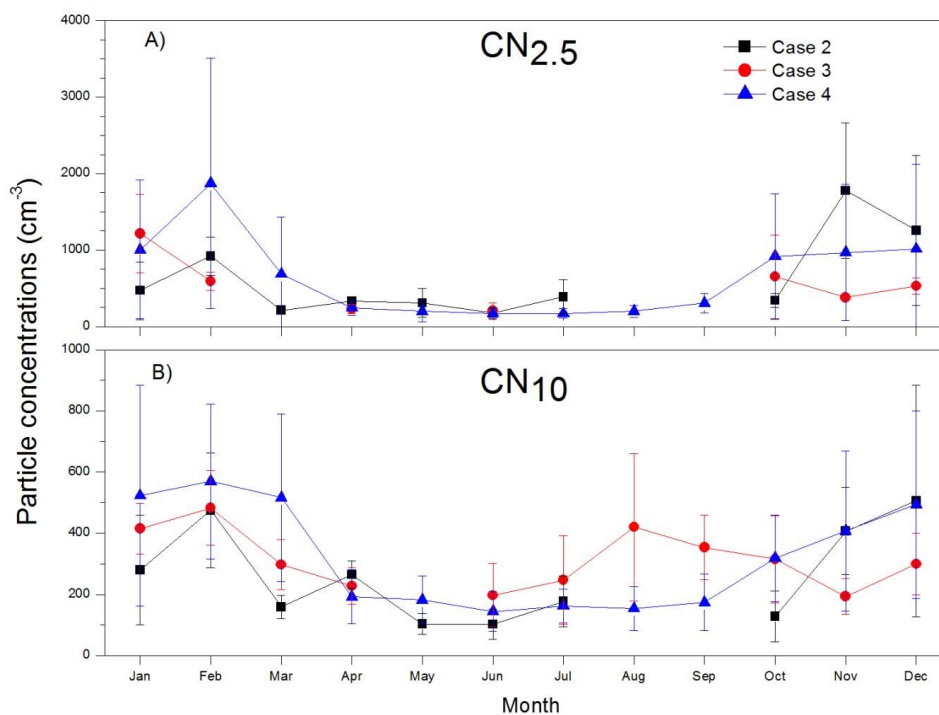


Figure 13. Seasonal variation of mean (a) CN_{2.5} and (b) CN₁₀ concentrations with a standard deviation depending on the air mass origin.

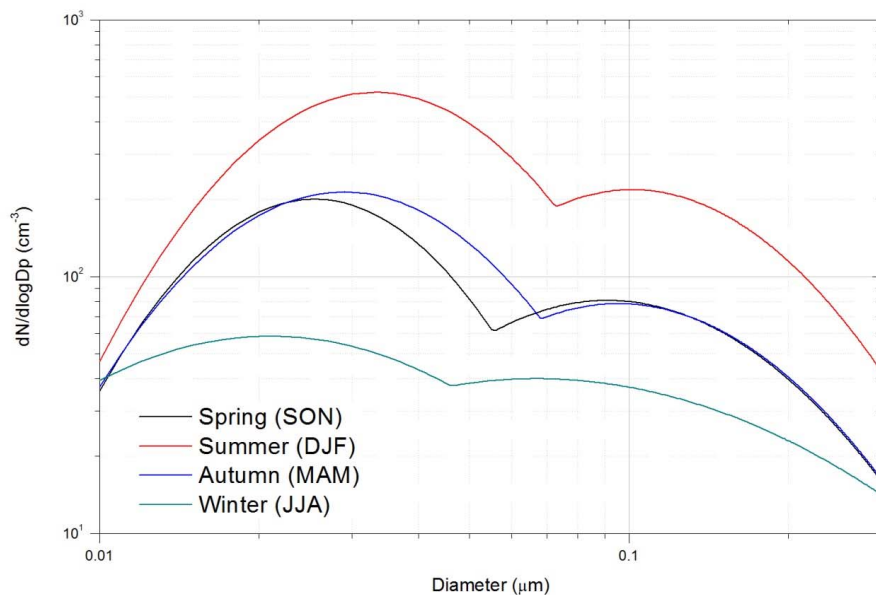


Figure 14. Seasonal lognormally fitted size distribution of aerosol particles originating from the South Pacific Ocean, ranging from 0.01 to 0.3 μm (Case 4).



Table 1. Summary of meteorology and aerosol data according to the origin and transport pathway of aerosol particles. Case 1, Case 2, Case 3, and Case 4 refer to the origin and pathway of the air masses from South America, South Atlantic Ocean, Antarctica and South Pacific Ocean, respectively.

	Overall	Case 1	Case 2	Case 3	Case 4
Wind speed (m s^{-1})	8.4 ± 1.8	2.6 ± 1.1	6.0 ± 1.5	6.7 ± 1.7	8.6 ± 1.8
Wind direction (deg)	237.2 ± 55.8	186.2 ± 20.7	155.9 ± 50.3	206.9 ± 52.3	242.7 ± 55.3
BC concentrations (ng m^{-3})	65.1 ± 29.2	122.2 ± 10.6	36.7 ± 14.2	65.6 ± 30.0	66.5 ± 29.5
CCN concentrations (cm^{-3})	129.7 ± 50.5	212.8 ± 50.2	146.0 ± 50.3	128.9 ± 34.9	128.7 ± 50.8
CN_{2.5} concentrations (cm^{-3})	737.3 ± 849.4	374.9 ± 64.4	605.3 ± 517.6	578.9 ± 377.3	751.2 ± 877.1
CN₁₀ concentrations (cm^{-3})	347.8 ± 229.1	358.8 ± 61.2	268.8 ± 173.9	331.9 ± 133.0	352.2 ± 234.9
Frequency		3	113	118	2407

5



Table 2. Seasonal size distribution lognormal fitting parameters for the Aitken and Accumulation mode of aerosol particles originating from a Case 4 scenario. N , σ , and D_g refer to the number concentrations, a standard deviation, and the geometric mean diameter, respectively.

	Aitken mode			Accumulation mode		
	N (cm^{-3})	σ	D_g (μm)	N (cm^{-3})	σ	D_g (μm)
Spring (SON)	112.010	1.655	0.026	53.873	1.939	0.094
Summer (DJF)	304.359	1.727	0.034	140.250	1.823	0.109
Autumn (MAM)	118.643	1.764	0.028	50.934	1.901	0.092
Winter (JJA)	49.164	2.296	0.023	44.780	2.827	0.086

5